Discerning in-situ performance of an EOR agent in the midst of geological uncertainty I Layer cake reservoir model

Fatemi, S. A.; Jansen, J. D.; Rossen, W. R.

DOI
10.1016/j.petrol.2017.08.021

Publication date
2017

Document Version
Final published version

Published in
Journal of Petroleum Science and Engineering

Journal of Petroleum Science and Engineering 158 (2017) 56–65

Contents lists available at ScienceDirect

Journal of Petroleum Science and Engineering

journal homepage: www.elsevier.com/locate/petrol

Discerning in-situ performance of an EOR agent in the midst of geological uncertainty I: Layer cake reservoir model

S.A. Fatemi *, J.D. Jansen, W.R. Rossen

Department of Geoscience and Engineering, Delft University of Technology, The Netherlands

ARTICLE INFO

Keywords:
Chemical flood
Uncertainty analysis
Geological uncertainty
EOR performance uncertainty
Reservoir simulation

ABSTRACT

An enhanced-oil-recovery (EOR) pilot test has multiple goals, among them to demonstrate oil recovery, verify the properties of the EOR agent in-situ, and provide the information needed for scale-up to an economic process. Given the complexity of EOR processes and the inherent uncertainty in the reservoir description, it is a challenge to discern the properties of the EOR agent in-situ in the midst of geological uncertainty. We propose a general workflow and present a case study to illustrate this challenge: a polymer EOR process in a 2D layer-cake reservoir. The polymer is designed to have a viscosity of 60 cp in-situ. There is uncertainty in the reservoir description, represented here by a range of values of Dykstra Parsons coefficient and different spatial arrangements of layers. We allow that the polymer process might fail in-situ and viscosity could be 20% of that intended. We test whether the signals of this difference at injection and production wells would be statistically significant in the midst of the geological uncertainty. Specifically, we compare the deviation caused by loss of polymer viscosity to the scatter caused by the geological uncertainty using the statistical 95% confidence interval. Among the signals considered, the 'rate of rise in injection pressure with polymer injection' and 'maximum injection pressure in the injector' give the most reliable indications of whether a polymer viscosity was maintained in-situ. If unintended and uncontrolled fracturing of the injection well is considered likely during polymer injection, however, injection pressure may be an unreliable indicator of in-situ polymer viscosity. In that case a diagnostic fracture-injection/falloff test could produce the needed indication of polymer viscosity in-situ. 'Polymer breakthrough time' and 'cumulative oil production at the end of process' give indications of polymer in-situ loss in some of the cases. With a more severe viscosity loss, e.g. 90% or worse, these signals give a statistically significant indication of loss of polymer viscosity in all of the cases.

1. Introduction

An EOR pilot test has multiple goals: to demonstrate oil recovery, verify the properties of the EOR agent in-situ, and provide the information needed for scale-up to an economic process. The first goal concerns whether the process achieves its overall objectives (oil recovery) in the given formation. Whether or not the first goal is reached, it is important to assess the process by the second criterion. This is important because a process that did not achieve the desired objectives in the given formation might be successful in another field if it demonstrates that it achieves its technical objectives. For example, the technical criteria for success for an EOR agent in-situ could be low interfacial tension (IFT) or low residual oil saturation for a surfactant process, a given mobility for a polymer process, etc. In a field pilot, one must determine the technical success of an EOR agent in the midst of geological uncertainty in the reservoir description while the EOR process is in progress.

Previous research has examined uncertainty in EOR process performance or uncertainty in the geological description, but not the two together. Studies on uncertainty in EOR process performance include Alkhatib and King (2015), Brown and Smith (1984), and Adepoju et al. (2017), examining surfactant-flood and polymer-flood processes. There have also been studies on the effect of geological heterogeneities and their uncertainty on how an EOR process performs. Heterogeneity and geological factors have different impacts on the various EOR processes, including polymer and alkaline-surfactant-polymer, thermal and gas-injection (miscible and immiscible) EOR. Studies of the effects of geological heterogeneity and uncertainty on EOR performance include Kumar et al. (2006), Chen et al. (2008), Popov et al. (2010), Rashid et al. (2010), Soleimani et al. (2011), Chiotoroiu et al. (2017), and Kumar et al. (2017).

* Corresponding author. Delft University of Technology, Department of Geoscience and Engineering, Stevinweg 1, 2628 CN Delft, The Netherlands.
E-mail address: s.a.fatemi@tudelft.nl (S.A. Fatemi).

http://dx.doi.org/10.1016/j.petrol.2017.08.021
Received 5 April 2017; Received in revised form 23 June 2017; Accepted 4 August 2017
Available online 7 August 2017

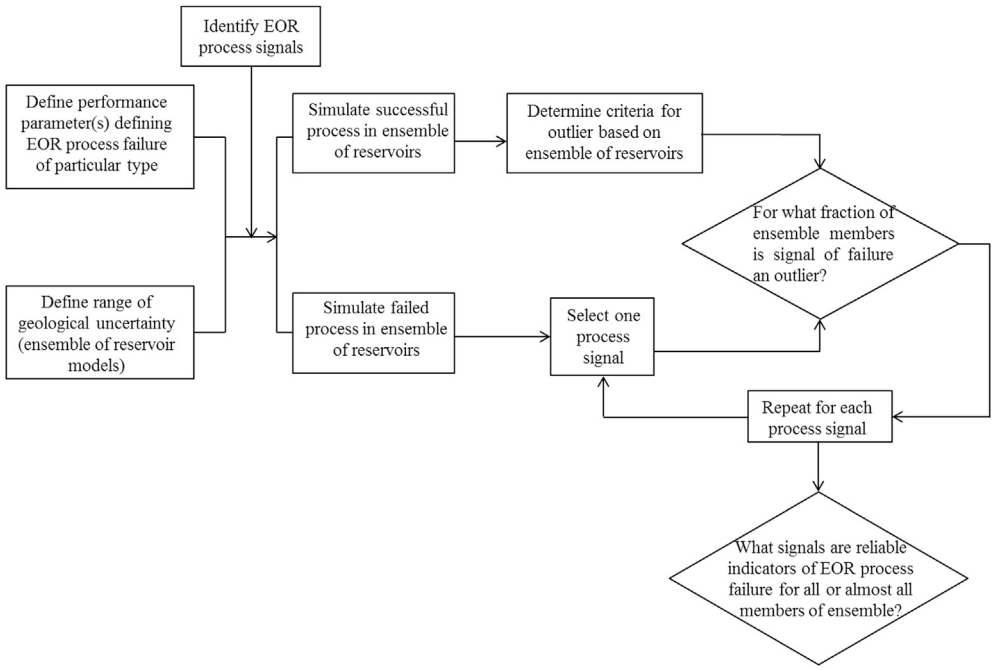

Fig. 1. Workflow to determine criteria to distinguish EOR process performance in-situ in the midst of geological uncertainties.

Table 1
Reservoir dimensions.

Description	Quantities	Units
Number of Grid Blocks (N_X, N_Y, N_Z)	25 × 1 × 5	–
Grid Block Size (Δx, Δy, Δz)	6.4 × 1 × 6.4	m
Total Dimensions	160 × 1 × 32	m
Porosity (φ)	0.3	

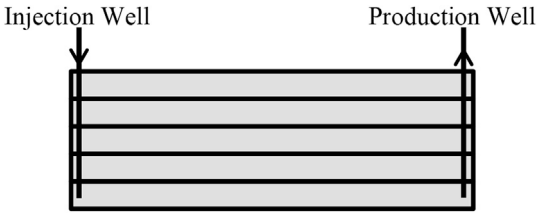

Fig. 2. The case study: a five-layer rectangular reservoir with one producer and one injector.

Table 2
Case-study reservoir and injection fluid properties.

Description	Quantities	Units
Water density	1000	kg/m^3
Oil density	900	kg/m^3
Water viscosity	1.00×10^{-3}	Pa.s
Oil viscosity	60.00×10^{-3}	Pa.s
Water compressibility	1.00×10^{-10}	bar^{-1}
Oil compressibility	1.00×10^{-10}	bar^{-1}
Initial Reservoir Pressure	85	bar

In this paper, we propose a workflow to discern the performance of the EOR agent in-situ in the midst of geological uncertainty. We further show how to implement the workflow in a case study to investigate the impact of both sources of uncertainty together in a statistical approach. We present a simple model to illustrate the issues involved: a polymer EOR process implemented in a 2D layer-cake reservoir. The polymer is intended to have a viscosity of 60 cp in-situ. Then, we allow that the polymer process might fail in-situ and viscosity could be 20% of that intended. This failure could be the result of mechanical degradation in surface facilities or on entering the perforations, faulty translation from laboratory-measured properties to properties in-situ, or faulty characterization of resident reservoir brine. Several of these adverse events would give different polymer properties in different regions of the reservoir. For simplicity, in this initial study we assume that throughout the reservoir polymer viscosity is less than that intended. We test whether the signals of this failure at the injection and production wells would be statistically significant in the midst of the geological uncertainty in the reservoir description. For a population of reservoirs representing geological uncertainty, we compare the deviation caused by loss of polymer viscosity to the scatter caused by the geological uncertainty using the 95% confidence interval statistical approach. Various signals are monitored to see which are the most reliable indications of whether a polymer viscosity was maintained in-situ. We further investigate the statistical significance of each signal. For this initial case study the

Table 3
Suggested ranges of values for a reservoir candidate for a polymer flooding (Dickson et al. (2010) and Saleh et al. (2014)).

	Suggested in Literature	Case Study
In-situ oil viscosity (cp)	10–1000	60
Average permeability, mD	>100 if (10<μ<100cp) >1000 if (100<μ < 1000cp)	1000
Oil Saturation (%)	>30%	90%

Table 4
Layer permeability values for V_{dp} = 0.6, 0.75 and 0.9; k_{avg} = 1000 md in all cases.

Permeability Values (md)			
Percentile	V_{dp} = 0.6	V_{dp} = 0.75	V_{dp} = 0.9
0.1	218	84	9
0.3	444	244	53
0.5	726	511	189
0.7	1189	1067	664
0.9	2423	3093	4086

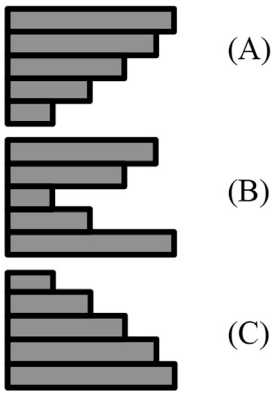

Fig. 3. Schematic of spatial ordering of layer permeabilities.

separate effects of adsorption, mixing with different brines in-situ, residual resistance factor, polymer degradation, shear-rate dependence (non-Newtonian behavior), permeability reduction and temperature have been ignored, except as they are represented indirectly in the loss of polymer viscosity.

2. Proposed workflow

Fig. 1 displays the key steps in discerning in-situ performance of an EOR process in the midst of geological uncertainty in a more organized structure. The left of the workflow shows two sources of uncertainty:

- Uncertainty in the performance of the EOR process itself, where we identify a key EOR performance parameter and its value for a successful EOR process and in a failure: for example, the intended, or design, value of polymer viscosity in-situ and its value if the process fails.
- Uncertainty in our knowledge of the subsurface, with the range of geological uncertainties represented by an ensemble of reservoir realizations.

The next step is to define and simulate the base case. A design EOR process is defined and simulated in the ensemble of geological representations. This design EOR process represents the successful intended EOR process. While an EOR process is in progress, there are a number of injection- or production-well data (signals) that reflect its performance in-situ. From the simulation results of the base case, we calculate the well signals of the design process. For each signal in the design process, based on the ensemble of reservoirs, we determine the 95% confidence interval (criteria for identifying an outlier). We then simulate what could represent a failed EOR process in the same ensemble of reservoirs (in this case study by dropping the design viscosity value to 20% of that intended). For each computed signal, we compare its value for the failed process to the confidence interval from the design process. When a given signal falls in the rejection-zone we label it as an outlier. If a signal reflects the process failure by being an outlier for all the reservoirs in the ensemble, it is a reliable indicator of process failure in the midst of geological uncertainty.

3. Case study

Table 1 presents the model dimensions and properties of the case study. The five-layer rectangular reservoir is shown in Fig. 2. Polymer-flood simulations were run with one injector and one producer, each penetrating the center of the first or last grid block in each layer. The producer bottom-hole pressure (BHP) is kept at 70 bars while the injector's BHP can go as high as 170 bars. The OOIP of the reservoir is 1382 m^3. A polymer solution of 1200 ppm, which gives the viscosity of 60 cp in-situ at 150 °F (based on the polymer-rheology algorithm in the simulator), is injected at a rate of 0.5 m^3/day. Polymer viscosity reduces injectivity, but unintended fracturing near the wellbore during polymer injection can increase injectivity. The extent of this unintended fracturing may not be known (Seright et al., 2009). Therefore, for simplicity, we account for an uncertain extent of injectivity improvement due to fracturing by allowing the injector BHP in the simulation to be greater than what one would expect to be applied in a polymer EOR process.

Table 2 presents the reservoir and injected fluid properties. Water, oil and polymer-slug viscosity are constants in the simulations. Our case study fits the criteria for a polymer EOR candidate based on the screening benchmarks suggested in the literature Alvarado and Manrique (2010), Dickson et al. (2010), and Saleh et al. (2014), as shown in Table 3.

3.1. Representation of uncertainty in polymer-flood performance

We represent uncertainty in process performance using two different values of polymer viscosity in-situ: 12 cp and 60 cp. As mentioned above, for simplicity in this initial study, various detailed influential mechanisms on the polymer viscosity in-situ are excluded. In our simulations, we represent the failure to attain the design viscosity in-situ by injecting the polymer concentration corresponding to 12 cp (400 ppm) instead of that corresponding to 60 cp (1200 ppm). Since we exclude adsorption from our study, this change in polymer concentration in the simulation

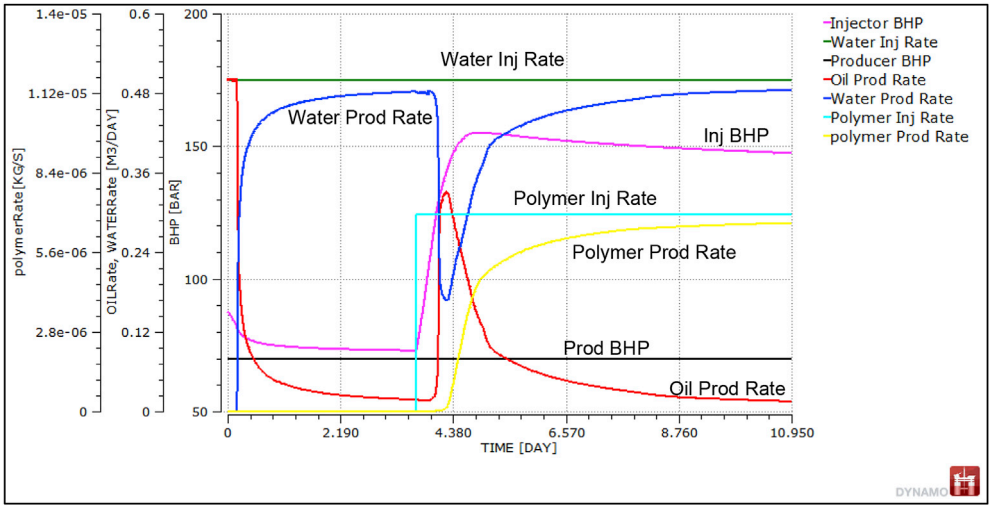

Fig. 4. Production/injection profile for the geological description corresponding to $V_{dp} = 0.9$ and layer ordering of schematic A.

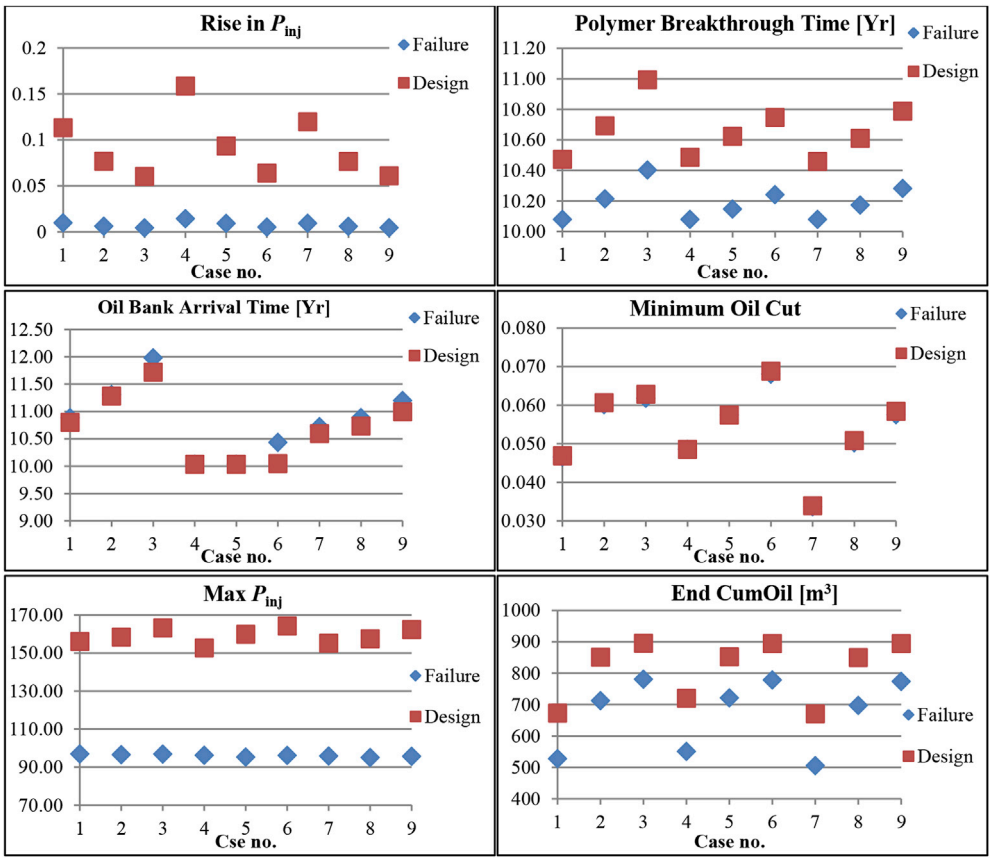

Fig. 5. Comparing signals of the process with 60 cp polymer viscosity (design) with the 12 cp polymer viscosity (failure).

Table 5
Signal values calculated for the nine geological cases with 60 cp polymer viscosity, with upper and lower bounds of the 95% confidence interval (CI+, CI—) for each signal.

Case no.	Perm. Distribution	*Vdp*	Rise in P_{inj}	Polymer BT [Yr]	Oil Bank Arrival Time [Yr]	Min. oil cut	Max Pinj [Bar]	Cumoil at End [m³]
1		**0.9**	0.113	10.47	10.80	0.047	156.00	672.87
2		**0.75**	0.077	10.69	11.28	0.061	158.34	850.90
3		**0.6**	0.060	10.99	11.72	0.063	163.21	894.80
4		**0.9**	0.159	10.49	10.03	0.049	152.64	720.13
5		**0.75**	0.093	10.62	10.03	0.057	159.84	852.03
6		**0.6**	0.064	10.75	10.05	0.069	164.15	894.17
7		**0.9**	0.120	10.46	10.60	0.034	155.17	670.63
8		**0.75**	0.077	10.61	10.73	0.051	157.53	849.76
9		**0.6**	0.061	10.79	10.99	0.058	162.31	894.04
	Mean		0.09	10.65	10.69	0.05	158.80	811.04
	STD		0.03	0.17	0.59	0.01	3.91	95.30
	t*@95%	2.308						
	CI +		0.17	11.06	12.06	0.08	167.82	1030.99
	CI -		0.01	10.25	9.33	0.03	149.78	591.09

does not retard the advance of the polymer bank.

Appendix A applies fractional-flow theory (Lake et al., 2014) to this polymer EOR process. It shows the incremental oil expected from a successful EOR process in 1D after 2 PV injection and loss in performance for the failed process. Fingering is not represented in this model, but the increase in mobility ratio at the shock suggests that the effects of heterogeneity would be worse in the failed process.

3.2. Representation of geological uncertainty

Petroleum engineers usually consider permeability heterogeneity the most important source of uncertainty in reservoir performance (Craig, 1993). Modeling of permeability heterogeneities is usually based on a stochastic description, and realizations of such models are input parameters to reservoir simulators (Langtangen, 1991). We therefore represent geological uncertainty with a number of realizations reflecting a range of reservoir properties.

Table 6
Discerning the process with 12 cp polymer viscosity from the case with 60 cp polymer viscosity.

Case no.	Perm. Distribution	*Vdp*	Rise in P_{inj}		Polymer BT [Yr]		Oil Bank Arrival Time [Yr]		Min. Oil Cut		Max P_{inj} [Bar]		End Cumoil [m^3]	
1		**0.9**	0.010	Outlier	10.08	Outlier	10.88	-	0.047	-	96.91	Outlier	527.5	Outlier
2		**0.75**	0.006	Outlier	10.21	Outlier	11.31	-	0.060	-	96.48	Outlier	712.3	-
3		**0.6**	0.004	Outlier	10.40	-	11.98	-	0.062	-	96.80	Outlier	780.6	-
4		**0.9**	0.014	Outlier	10.08	Outlier	10.03	-	0.049	-	96.19	Outlier	550.9	Outlier
5		**0.75**	0.009	Outlier	10.15	Outlier	10.03	-	0.057	-	95.24	Outlier	721.1	-
6		**0.6**	0.005	Outlier	10.24	Outlier	10.43	-	0.068	-	96.12	Outlier	778	-
7	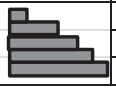	**0.9**	0.009	Outlier	10.08	Outlier	10.72	-	0.034	-	95.82	Outlier	505.4	Outlier
8		**0.75**	0.006	Outlier	10.17	Outlier	10.88	-	0.050	-	95.02	Outlier	697.3	-
9		**0.6**	0.005	Outlier	10.28	-	11.20	-	0.057	-	95.64	Outlier	773.7	-

In this layer-cake model, each layer has a different permeability. The distribution of permeability values follows a log-normal distribution. The log-normal distribution has often been used to describe the permeability distribution of heterogeneous reservoirs (Dykstra and Parsons, 1956) (Jensen et al., 2000), and (Lake et al., 2014). The degree of heterogeneity of a reservoir is often characterized by the dimensionless Dykstra-Parsons coefficient of permeability variation (V_{dp}). A homogeneous reservoir has a V_{dp} approaching zero, while an extremely heterogeneous reservoir would have a V_{dp} approaching one. A log-normal permeability distribution can be characterized by this coefficient and an average permeability (Craig, 1993) and (Hirasaki, 1984). To generate the permeability values for the five layers we use the inverse cumulative distribution function (CDF) of the log-normal distribution. Specifically, the permeability values are drawn from the 10%, 30%, 50%, 70% and 90% percentiles of the CDF. We adjust the magnitudes of the values so that all three distributions have the same arithmetic average permeability (K_{avg}). Therefore in single-phase flow injectivity would be the same for all the nine cases. Table 4 shows the permeability values generated for $V_{dp} = 0.6$, 0.75 and 0.9.

We assume three spatial distributions of permeability: specifically, from top to bottom, high-permeability to low-permeability, low-permeability to high-permeability, and a distribution with the lowest permeability in the middle. Fig. 3 shows schematically how layer permeabilities are ordered. Three Dykstra Parsons coefficients and three spatial arrangements of layers give nine different geological representations, to be used in simulations with two different polymer-flood in-situ viscosities.

This initial study illustrates the interplay between geological and process uncertainty using an extreme extent of geological uncertainty at the wellbore. A single successful well log could resolve much of this uncertainty. In the context of a layer-cake model, the range of layer permeabilities in our model represents the much larger uncertainty in reservoir properties between wells.

Appendix B compares the competing effects of heterogeneity, gravity and arrangement of layers for the waterflood. Gravity reduces sweep efficiency in this case if the high-permeability layers are on the bottom, but is not as important as heterogeneity.

3.3. Development scenario and procedure

We run the polymer-flood simulations using Shell's in-house simulator MoReS (Van Doren et al., 2011). In each simulation, ten years of water injection is followed by twenty years of polymer-slug injection. A production/injection profile for one case is shown in Fig. 4.

As shown in Fig. 4, water is injected for 10 years, and it breaks through early in the waterflood. A polymer slug is then injected and causes a rise in injection pressure and, later, incremental oil recovery, reflected in the rise in oil production shown in the red line. There are a number of signals that reflect the effectiveness of polymer:

- Polymer breakthrough time, years (Polymer BT)
- Rate of rise in P_{inj} upon polymer injection in six months, bars (Rise in P_{inj})
- Minimum oil cut (Min. oil cut)
- Time of initial increase in oil production rate, years (Oil Bank Arrival Time)
- Max injection pressure, bars (Max P_{inj})
- Cumulative oil production at end of process, m^3 (End Cumoil)

4. Results

We allow that the polymer process might fail in-situ and viscosity could be 20% that intended.

Fig. 5 shows a plot of the signal values of nine reservoir descriptions for a polymer viscosity in-situ of 60 cp and those for a viscosity of 12 cp. Fig. 5 shows that it is hardest to distinguish EOR process failure if the reservoir is relatively homogeneous (case 3, 6 and 8) and easiest if it lies toward the heterogeneous end of the spectrum of possibilities (cases 1, 4 and 7). Increasing reservoir heterogeneity produces results similar to EOR process failure in-situ: earlier polymer breakthrough and reduced cumulative oil recovery.

Comparing the signals listed above we test whether the signals of this viscosity difference would be statistically significant (using the 95% confidence interval) in the midst of the geological uncertainty, represented by the nine reservoir descriptions. Specifically, we calculate the 95% confidence interval for each signal for the nine geological cases with 60 cp polymer viscosity. Refer to Appendix C for more details on how to calculate the ***t***-distribution 95% confidence interval. The results are shown in Table 5.

For each reservoir description we then ask if the given signal with 12 cp polymer viscosity lies in the rejection zone of the 95% confidence interval. If the answer is yes, then the signal is an outlier and failure of polymer in-situ is discernible in the midst of geological uncertainty. Table 6 shows the signal values for the cases with an in-situ viscosity of 12 cp. Next to each column with this signal value, a second column checks if the individual value falls in the rejection zone of results with 60 cp viscosity from Table 5. If the signal value falls in the rejection, it is labelled as an "Outlier" in the adjacent column (meaning the signal can be distinguished in the midst of geological uncertainty). Otherwise the entry is left as blank in the adjacent column, meaning the signal cannot be distinguished from geological uncertainty.

Of the signals considered, there are two columns labelled entirely as outliers. One could discern the effect of viscosity with confidence in every case based on the 'rate of rise in P_{inj} in six months' and 'max injection pressure'. These two signals could discern the failure of the polymer in-situ in the midst of geological uncertainty. In both cases, the rise in pressure is less than with the greater polymer viscosity, as expected. 'Polymer breakthrough time' could discern the effect of viscosity in majority of the cases excluding the next homogeneous case. For

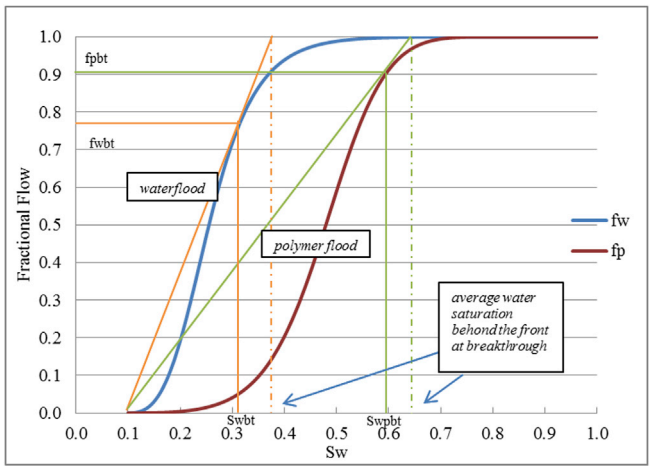

Fig. A.1. Graphical construction of water and polymer fractional flow in secondary mode for the design polymer in-situ viscosity of 60 cp.

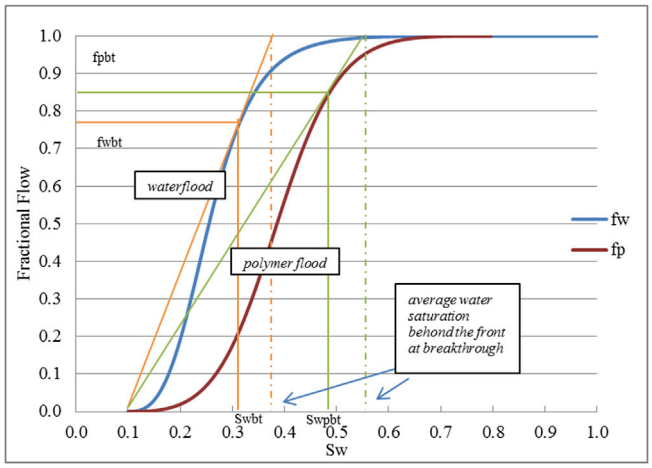

Fig. A.2. Graphical construction of water and polymer fractional flow in secondary mode for the reduced polymer in-situ viscosity of 12 cp.

'cumulative oil production at end of simulation', failure can be discerned only in the most heterogeneous cases.

In this case study, we deal with an extreme reservoir heterogeneity description. Only when there is a severe in-situ viscosity loss is the difference in signals between the two populations statistically significant. Refer to Appendix D for more results for different extent of in-situ viscosity loss. When there is a 10% viscosity loss, only the 'max P_{inj}' signal can discern the more heterogeneous cases. As the extent of viscosity loss increases, this effect is more statistically significant among the signals. In the very extreme in-situ viscosity loss of 90%, 'rate of rise in P_{inj} in six months', 'polymer breakthrough time' and 'max injection pressure' could discern the failure of the polymer in-situ in the midst of geological uncertainty in all of the cases and 'cumulative oil production at end of simulation' discerns the effect in the more heterogeneous cases.

Table A.1
Recoveries after polymer breakthrough for the design viscosity case versus reduced viscosity.

	Waterflood	Design viscosity, 60 cp	Reduced viscosity, 12 cp
Oil recovery at breakthrough, %	28%	0.55	0.46
Mobility ratio at shock front[a]	1.47	0.12	0.76
Fraction of movable oil recovered at 2 PV injection[b]		0.97	0.92

[a] Mobility behind the front divided by mobility ahead of the front.
[b] $(S_{wavg} - S_{wc})/(1 - S_{wc} - S_{or})$.

5. Conclusions and discussion

- We offer a workflow and a simple initial study of a polymer flood to illustrate the issues involved in attempting to distinguish EOR process performance from well data in the midst of geological uncertainty.
- Among the signals considered here, the rate of rise in injection pressure upon polymer injection and maximum pressure in the injection well give the most reliable indications of whether polymer viscosity was maintained in-situ. Given the chances of fracturing of the injection well (Seright et al., 2009), especially if the extent of this fracturing is unknown, injection pressure could be an unreliable indicator of in-situ polymer viscosity injection. In that case a diagnostic fracture-injection/falloff test could substitute for the well pressure data (Craig and Jackson, 2017).
- Among the other signals considered, it was hardest to distinguish failure of the EOR process in reservoirs that, among the ensemble of equi-probable reservoirs, were relatively homogeneous. For these cases waterflood by itself performed relatively well; the failure of the EOR process was hard to distinguish from the possibility of greater reservoir heterogeneity. Failure was easiest to identify if the actual reservoir was among the more heterogeneous cases considered possible. In that case the additional loss in performance from failure of the EOR process produced a result outside the confidence interval.
- Previous studies that considered the effect of geological uncertainty on EOR process performance, establish the range of outcomes for a process that performs in-situ as designed. In effect, they establish the confidence interval beyond which a failed EOR process could be identified.
- The range of geological uncertainty in this initial case study could be viewed as extreme. We assume that injectivity is known but that very little is known about the extent of reservoir heterogeneity, even at the wells. On the other hand, the extent of failure of the polymer in-situ, i.e. a loss of viscosity by a factor of 5, could be considered extreme as well. Moreover, we consider a two-well situation whereas in a multi-well setting the effect of viscosity changes may result in different signals in the various wells. Further study should include more realistic geological descriptions and polymer mechanisms and the effect of including more wells.

Acknowledgment

This research was carried out within the context of the Recovery Factory programme, a joint project of Shell Global Solutions International and Delft University of Technology. The authors wish to thank Shell Global Solutions International B.V. for permission to publish this work.

Appendix A. Fractional-flow theory in polymer flooding

It is useful to perform a 1D fractional-flow analysis of a reservoir to identify whether is suitable for a particular recovery process before undertaking a detailed reservoir simulation study. One of the simplest and most widely used methods of estimating the displacement efficiency in an immiscible displacement process is the Buckley-Leverett method (Fanchi, 2005), (Craft et al., 1991), (Dake, 2001), and (Lake et al., 2014). Our purpose here is to compare the displacement efficiency in 1D for the design polymer flood versus the reduced-viscosity polymer flood. The polymer-oil fractional flow

curve is constructed and shown in Fig. A1 and Fig. A2 for two cases, one with the polymer design viscosity of 60 cp and the other with reduced polymer viscosity of 12 cp. Polymer injection reduces the mobility ratio, causing the $f_w(S_w)$ curves to shift to the right. The greater the polymer viscosity the more the polymer-flood curve shifts to the right. The recovery of the 1D polymer flood at polymer breakthrough, mobility ratio at shock front and recovery at 2 PV injection can be extracted from the fractional-flow diagram, as shown in Table A.1. Although the case shown in Fig. A1 and Fig. A2 is a secondary polymer flood, the mobility ratio at the shock front and recovery after 2 PV injection would be identical for polymer floods in secondary and tertiary modes.

Table A.1 shows that even in a homogenous 1D reservoir without gravity segregation there is less oil recovered at polymer breakthrough and after 2 PV injection with the lower viscosity. The mobility ratio at the shock front is smaller for the design viscosity than the reduced viscosity, which suggests a better mobility control and more uniform sweep in a 2D heterogeneous reservoir for the design viscosity case.

Appendix B. Effect of gravity

Gravitational force affects crossflow in communicating layers. These forces tend to increase the water saturation on the bottom layers (Craig, 1993). Fig. 4 shows the oil recovery during the waterflood phase of our case study for different levels of heterogeneity and layer ordering. As this figure shows, arrangement of the layers plays a less-important role than the effect of heterogeneity. This suggests gravity is not dominant on our case-study results. With the high-permeable layer on the top and the permeability decreasing with depth (schematic A in Fig. 3), gravity tends to increase oil recovery. Gravity reduces oil recovery for the permeability arrangement in which permeability increases with depth (schematic C in Fig. 3). If gravity was not relevant at all, permeability arrangements in schematics A and C would behave identically, but, as Fig. 4 shows, oil recovery is not the same for the two permeability arrangements; hence the arrangement of layers matters in this case study.

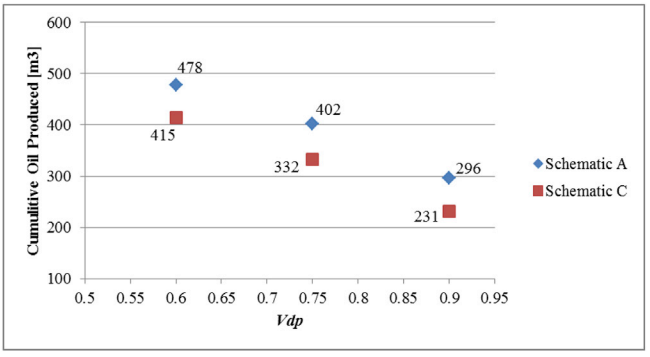

Fig. B.1. Effect of gravity on Cumulative Oil Production (after 10 years of waterflood) in different permeability arrangements.

Appendix C. Confidence intervals based on the *t*-distribution

The confidence interval is an estimate of the range in which a given percentage of a statistical population lies. If a datum lies outside the 95% confidence interval, there is less than 5% chance that a randomly selected member of that population would be so far from the population mean. Though imperfect, this is a standard test for the likelihood that a new case is derived from the same statistical population as the original sample (Hawkins, 1980).

The confidence interval (CI) is inferred from the mean, X_{avg}, and standard deviation, σ, of a sample from the population using the t statistic:

$$CI = X_{avg} \pm t^* \sigma \qquad (C.1)$$

The value of t^* for the 95% confidence interval for a set of 9 data samples (8 degrees of freedom) is 2.306.

Appendix D

Here we present different scenarios of polymer in-situ viscosity loss (10%, 20%, 50%, 60%, 70% and 90%) and the associated effect on different well signals.

Table D.1
Discerning the process with 54 cp polymer viscosity from the case with 60 cp polymer viscosity.

Perm. Distribution	*Vdp*	Rise in P_{inj}		Polymer BT [Yr]		Oil Bank Arrival Time [Yr]		Min. Oil Cut		Max P_{inj} [Bar]		End Cumoil [m^3]	
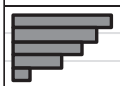	**0.9**	0.101	-	10.23	Outlier	10.73	-	0.047	-	146.94	Outlier	658.56	-
	0.75	0.068	-	10.36	-	11.27	-	0.061	-	148.48	Outlier	839.93	-
	0.6	0.053	-	10.55	-	11.84	-	0.063	-	152.68	-	886.15	-
	**0.9**	0.144	-	10.24	Outlier	10.03	-	0.049	-	143.32	Outlier	706.09	-
	0.75	0.084	-	10.31	-	10.03	-	0.057	-	149.67	Outlier	841.44	-
	0.6	0.056	-	10.39	-	10.05	-	0.069	-	153.67	-	885.46	-
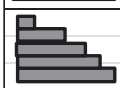	**0.9**	0.106	-	10.24	Outlier	10.60	-	0.034	-	145.89	Outlier	655.93	-
	0.75	0.068	-	10.32	-	10.80	-	0.051	-	147.55	Outlier	838.32	-
	0.6	0.054	-	10.43	-	11.10	-	0.058	-	151.72	-	885.27	-

Table D.2
Discerning the process with 48 cp polymer viscosity from the case with 60 cp polymer viscosity.

Perm. Distribution	*Vdp*	Rise in P_{inj}		Polymer BT [Yr]		Oil Bank Arrival Time [Yr]		Min. Oil Cut		Max P_{inj} [Bar]		End Cumoil [m^3]	
	**0.9**	0.089	-	10.21	Outlier	10.79	-	0.047	-	137.92	Outlier	642.71	-
	0.75	0.060	-	10.34	-	11.21	-	0.061	-	138.70	Outlier	826.72	-
	0.6	0.046	-	10.53	-	11.79	-	0.063	-	142.27	Outlier	876.04	-
	**0.9**	0.129	-	10.22	Outlier	10.03	-	0.049	-	134.69	Outlier	689.96	-
	0.75	0.075	-	10.29	-	10.03	-	0.057	-	139.56	Outlier	828.94	-
	0.6	0.049	-	10.38	-	10.05	-	0.069	-	143.27	Outlier	875.18	-
	**0.9**	0.093	-	10.22	Outlier	10.60	-	0.034	-	136.70	Outlier	639.32	-
	0.75	0.059	-	10.30	-	10.79	-	0.051	-	137.66	Outlier	824.62	-
	0.6	0.047	-	10.41	-	11.05	-	0.058	-	141.24	Outlier	874.79	-

Table D.3
Discerning the process with 30 cp polymer viscosity from the case with 60 cp polymer viscosity.

Perm. Distribution	*Vdp*	Rise in P_{inj}		Polymer BT [Yr]		Oil Bank Arrival Time [Yr]		Min. Oil Cut		Max P_{inj} [Bar]		End Cumoil [m^3]	
	**0.9**	0.05	-	10.17	Outlier	10.84	-	0.047	-	122.34	Outlier	610.89	-
	0.75	0.033	-	10.30	-	11.29	-	0.060	-	122.25	Outlier	796.56	-
	0.6	0.025	-	10.48	-	11.83	-	0.062	-	124.65	Outlier	852.97	-
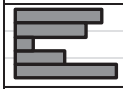	**0.9**	0.074	-	10.17	Outlier	10.03	-	0.049	-	120.71	Outlier	655.19	-
	0.75	0.043	-	10.24	Outlier	10.03	-	0.057	-	122.14	Outlier	801.46	-
	0.6	0.027	-	10.33	-	10.05	-	0.069	-	125.32	Outlier	851.74	-
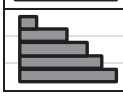	**0.9**	0.052	-	10.17	Outlier	10.72	-	0.034	-	121.10	Outlier	605.55	-
	0.75	0.033	-	10.26	-	10.87	-	0.051	-	121.02	Outlier	792.84	-
	0.6	0.026	-	10.36	-	11.10	-	0.058	-	123.48	Outlier	851.02	-

Table D.4
Discerning the process with 24 cp polymer viscosity from the case with 60 cp polymer viscosity.

Perm. Distribution	*Vdp*	Rise in P_{inj}		Polymer BT [Yr]		Oil Bank Arrival Time [Yr]		Min. Oil Cut		Max P_{inj} [Bar]		End Cumoil [m^3]	
	**0.9**	0.028	-	10.14	Outlier	10.79	-	0.047	-	115.43	Outlier	593.7	-
	0.75	0.018	-	10.27	-	11.23	-	0.060	-	115.04	Outlier	778.74	-
	0.6	0.014	Outlier	10.46	-	11.88	-	0.062	-	116.86	Outlier	839.14	-
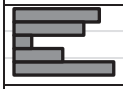	**0.9**	0.042	-	10.14	Outlier	10.03	-	0.049	-	114.10	Outlier	634.75	-
	0.75	0.025	-	10.21	Outlier	10.03	-	0.057	-	114.29	Outlier	785.28	-
	0.6	0.015	-	10.30	-	10.06	-	0.069	-	117.21	Outlier	837.75	-
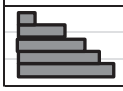	**0.9**	0.029	-	10.15	Outlier	10.69	-	0.034	-	114.18	Outlier	585.61	Outlier
	0.75	0.018	-	10.23	Outlier	10.72	-	0.051	-	113.72	Outlier	773.88	-
	0.6	0.014	Outlier	10.34	-	11.09	-	0.058	-	115.59	Outlier	836.73	-

Table D.5
Discerning the process with 18 cp polymer viscosity from the case with 60 cp polymer viscosity.

Perm. Distribution	*Vdp*	Rise in P_{inj}		Polymer BT [Yr]		Oil Bank Arrival Time [Yr]		Min. Oil Cut		Max P_{inj} [Bar]		End Cumoil [m^3]	
	**0.9**	0.016	-	10.12	Outlier	10.90	-	0.047	-	102.96	Outlier	552.59	Outlier
	0.75	0.011	Outlier	10.25	-	11.27	-	0.060	-	102.26	Outlier	737.26	-
	0.6	0.008	Outlier	10.46	-	12.02	-	0.062	-	103.01	Outlier	803.76	-
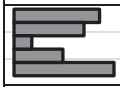	**0.9**	0.025	-	10.12	Outlier	10.03	-	0.049	-	101.69	Outlier	583.49	Outlier
	0.75	0.015	-	10.18	Outlier	10.03	-	0.057	-	100.62	Outlier	745.85	-
	0.6	0.009	Outlier	10.28	-	10.06	-	0.068	-	102.65	Outlier	801.84	-
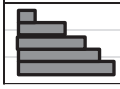	**0.9**	0.016	-	10.13	Outlier	10.71	-	0.034	-	101.74	Outlier	535.88	Outlier
	0.75	0.010	Outlier	10.21	Outlier	10.88	-	0.050	-	100.82	Outlier	728.46	-
	0.6	0.008	Outlier	10.32	-	11.14	-	0.058	-	101.74	Outlier	799.54	-

Table D.6
Discerning the process with 9 cp polymer viscosity from the case with 60 cp polymer viscosity.

Perm. Distribution	*Vdp*	Rise in P_{inj}		Polymer BT [Yr]		Oil Bank Arrival Time [Yr]		Min. Oil Cut		Max P_{inj} [Bar]		End Cumoil [m^3]	
	**0.9**	0.007	Outlier	9.93	Outlier	10.88	-	0.046	-	90.93	Outlier	500.74	Outlier
	0.75	0.004	Outlier	10.07	Outlier	11.34	-	0.060	-	90.85	Outlier	682.68	-
	0.6	0.003	Outlier	10.26	-	12.05	-	0.062	-	91.02	Outlier	752.26	-
	**0.9**	0.010	Outlier	9.93	Outlier	10.03	-	0.049	-	90.92	Outlier	513.71	Outlier
	0.75	0.007	Outlier	9.99	Outlier	10.03	-	0.057	-	89.96	Outlier	691.27	-
	0.6	0.004	Outlier	10.08	Outlier	10.60	-	0.068	-	90.17	Outlier	749.36	-
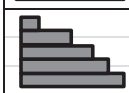	**0.9**	0.006	Outlier	9.94	Outlier	10.77	-	0.034	-	90.02	Outlier	470.93	Outlier
	0.75	0.004	Outlier	10.02	Outlier	10.92	-	0.050	-	89.32	Outlier	654.64	-
	0.6	0.003	Outlier	10.12	Outlier	11.31	-	0.057	-	89.79	Outlier	740.29	-

Table D.7
Discerning the process with 6 cp polymer viscosity from the case with 60 cp polymer viscosity.

Perm. Distribution	*Vdp*	Rise in P_{inj}		Polymer BT [Yr]		Oil Bank Arrival Time [Yr]		Min. Oil Cut		Max P_{inj} [Bar]		End Cumoil [m^3]	
	**0.9**	0.005	Outlier	9.88	Outlier	11.01	-	0.046	-	87.56	Outlier	442.36	Outlier
	0.75	0.003	Outlier	10.01	Outlier	11.53	-	0.059	-	87.49	Outlier	585.12	Outlier
	0.6	0.002	Outlier	10.21	Outlier	12.27	Outlier	0.061	-	87.42	Outlier	675.11	-
	**0.9**	0.006	Outlier	9.87	Outlier	10.03	-	0.049	-	87.38	Outlier	413.58	Outlier
	0.75	0.005	Outlier	9.94	Outlier	10.03	-	0.057	-	87.46	Outlier	589.29	Outlier
	0.6	0.003	Outlier	10.03	Outlier	10.91	-	0.066	-	87.34	Outlier	662.27	-
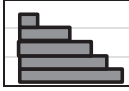	**0.9**	0.005	Outlier	9.88	Outlier	10.98	-	0.033	-	87.36	Outlier	370.96	Outlier
	0.75	0.003	Outlier	9.97	Outlier	11.13	-	0.050	-	87.28	Outlier	531.38	Outlier
	0.6	0.002	Outlier	10.08	Outlier	11.55	-	0.056	-	88.51	Outlier	632.29	-

References

Adepoju, O.O., Hussein, H., Chawathe, A., 2017. Assessment of chemical performance uncertainty in chemical EOR simulations. In: SPE Reservoir Simulation Conference. Society of Petroleum Engineers, Montgomery, Texas, USA.

Alkhatib, A.M., King, P.R., 2015. The use of the least-squares probabilistic-collocation method in decision making in the presence of uncertainty for chemical-enhanced-oil-recovery processes. SPE-84372-MS 20 (4).

Alvarado, V., Manrique, E., 2010. Enhanced Oil Recovery Field Planning and Development Strategies. Elsevier, UK.

Brown, C.E., Smith, P.J., 1984. The evaluation of uncertainty in surfactant EOR performance prediction. In: SPE Annual Technical Conference and Exhibition. Society of Petroleum Engineers, Houston, Texas.

Chen, Q., Gerritsen, M.G., Kovscek, A.R., 2008. Effects of reservoir heterogeneities on the steam-assisted gravity-drainage process. SPE Reserv. Eval. Eng. 11 (5).

Chiotoroiu, M.-M., Peisker, J., Clemens, T., Thiele, M., 2017. Forecasting incremental oil production of a polymer-pilot extension in the Matzen field including quantitative uncertainty assessment. SPE Reserv. Eval. Eng. Preprint(Preprint), SPE-179546-PA.

Craft, B.C., Hawkins, M., Terry, R.E., 1991. Applied Petroleum Reservoir Engineering. Prentice Hall, New Jersy, USA.

Craig, D.P., Jackson, R.A., 2017. Calculating the volume of reservoir investigated during a fracture-injection/falloff test DFIT. In: SPE Hydraulic Fracturing Technology Conference and Exhibition. Society of Petroleum Engineers, The Woodlands, Texas, USA.

Craig, F.F., 1993. The Reservoir Engineering Aspects of Waterflooding, second ed. Society of Petroleum Engineers, USA. SPE Monograph Series, 3.

Dake, L.P., 2001. Practice of Reservoir Engineering Developments in Petroleum Science. Developments in Petroleum Science, vol. 36. Elsevier Science, USA, 572 pp.

Dickson, J.L., Dios, A.L., Wylie, P.L., 2010. Development of improved hydrocarbon recovery screening methodologies. In: SPE Improved Oil Recovery Symposium. Society of Petroleum Engineers, Tulsa, Oklahoma, USA.

Dykstra, H., Parsons, R.L., 1956. The Prediction of Oil Recovery by Water Flood.

Fanchi, J.R., 2005. Principles of Applied Reservoir Simulation. Elsevier, USA.

Hawkins, D.M., 1980. Identification of Outliers. Monographs on Applied Probability and Statistics. Springer Netherlands.

Hirasaki, G.J., 1984. Properties of Log-Normal Permeability Distribution for Stratified Reservoirs. Society of Petroleum Engineers.
Jensen, J., Lake, L.W., Corbett, P., Goggin, D., 2000. Statistics for Petroleum Engineers and Geoscientists, vol. 2. Elsevier, USA.
Kumar, M., Hoang, V., Satik, C., Rojas, D., 2006. High-mobility-ratio-waterflood Performance Prediction: Challenges and New Insights.
Kumar, R., Shankar, V., Batra, S.K., Kumar, A., 2017. Effect of reservoir heterogeneities and model uncertainties on prediction versus actual field behavior- a case study. In: SPE Oil and Gas India Conference and Exhibition. Society of Petroleum Engineers, Mumbai, India.
Lake, L.W., Johns, R., Rossen, W.R., Pope, G., 2014. Fundamentals of Enhanced Oil Recovery. Society of Petroleum Engineers, USA.
Langtangen, H.P., 1991. Sensitivity analysis of an enhanced oil recovery process. Appl. Math. Model. 15 (9), 467–474.
Popov, Y., et al., 2010. Thermal properties of formations from core analysis: evolution in measurement methods, equipment, and experimental data in relation to thermal EOR. In: Canadian Unconventional Resources and International Petroleum Conference. Society of Petroleum Engineers, Calgary, Alberta, Canada.
Rashid, B., Muggeridge, A., Bal, A.L., Williams, G.J.J., 2010. Quantifying the impact of permeability heterogeneity on secondary-recovery performance. In: SPE Annual Technical Conference and Exhibition. Society of Petroleum Engineers, Florence, Italy.
Saleh, L.D., Wei, M., Bai, B., 2014. Data analysis and updated screening criteria for polymer flooding based on oilfield data. SPE Reserv. Eval. Eng. 17 (1).
Seright, R.S., Seheult, J.M., Talashek, T., 2009. Injectivity characteristics of EOR polymers. SPE J. Pap. 12 (5).
Soleimani, A., et al., 2011. Impact of fluvial geological characteristics on EOR screening of a large heavy oil field. In: SPE Enhanced Oil Recovery Conference. Society of Petroleum Engineers, Kuala Lumpur, Malaysia.
Van Doren, J., Douma, S.G., Wassing, L.B.M., Kraaijevanger, J.F.B.M., Zwart, A.H.D., 2011. Adjoint-based optimization of polymer flooding. In: SPE Enhanced Oil Recovery Conference. Society of Petroleum Engineers, Kuala Lumpur, Malaysia.